

## Case Report

# Characterization of a Thermoelectric Generator (TEG) System for Waste Heat Recovery

Oswaldo Hideo Ando Junior \*, Nelson H. Calderon and Samara Silva de Souza

Department of Renewable Energies, UNILA, Federal University of Latin American Integration,  
Av. Sílvio Américo Sasdelli, 1842 Foz do Iguaçu-PR, Brazil; nchcalderon@gmail.com (N.H.C.);  
saengquimica@gmail.com (S.S.d.S.)

\* Correspondence: oswaldo.junior@unila.edu.br; Tel.: +55-045-3529-2138

Received: 14 May 2018; Accepted: 1 June 2018; Published: 14 June 2018



**Abstract:** This paper presents the development and characterization of a thermoelectric generator (TEG) system for waste heat recovery to low temperature in industrial processes. The relevance of this mode of electric energy harvest is that it is clean energy and it depends only on the capture of losses. These residual energies from industrial processes are, in principle, released into the environment without being exploited. With the proposed device, the waste energy will not be released into the environment and will be used for electrical generation, which is useful for heat production. The characterization of TEGs that are used a data-acquisition system have measured data for the voltage, current, and temperature, in real-time, for temperatures down to 200 °C without signal degradation. As a result, the measured data has revealed an open circuit voltage of  $V_{OC} = 0.4306 \times \Delta T$ , internal resistance of  $R_0 = 9.41 \, \Omega$ , with tolerance  $\Delta R_{int} = \pm 0.77 \, \Omega$ , where  $R_{int} = 9.41 \pm 0.77 \, \Omega$ . The measurements were made on the condition that the maximum output was obtained at a temperature gradient of  $\Delta T = 80 \, ^\circ\text{C}$ , resulting in a maximum power gain of  $P_{out} \approx 29 \, \text{W}$ .

**Keywords:** thermoelectricity; energy harvest; green energy; seebeck effect; cogeneration

## 1. Introduction

The energy issue and the demand for alternative sources, which are necessary to reduce the dependency on fossil fuels, are vital for all countries. Currently, electricity is considered a commodity for the development of a country, providing social and economic growth. However, there is an energy crisis that has evidenced the limits of the energy supply to meet the growing demand [1,2]. Therefore, it is important to seek new alternative sources that stand out as environmentally sustainable solutions, so as to diversify the energy matrix and thus minimize the environmental impacts, by prioritizing the substitution by renewable sources [3].

Nowadays, much has been discussed about clean and renewable energy sources, and consequently, the power that has been obtained from the waste heat recovery appears as an alternative, within renewable energy. This new technology includes the development of thermoelectric materials and applied systems, for instance, the wall of conventional furnaces, cooling of heat pipes, devices based on structured deposited, turbo compounding, Rankine and Brayton electric utilities, thermochemical recuperation, in-cylinder waste heat recovery, and improvement of cogeneration systems; which are all used for energy harvest using solid state thermoelectric devices [4–15]. The use of thermoelectric generation brings certain advantages, such as high durability, high precision, and reduced size, besides being an excellent way of collecting residual thermal energy, which means it is a clean energy cogeneration [16–20].

The research has been mainly focused on the investigation for high performance thermoelectric materials (especially resorting to nanostructures), for instance, Half-Heusler based semiconducting

intermetallic compounds and Graded Germanium–Lead Chalcogenide [20,21]. For example, American researchers have identified an important variation in the performance of the existing thermoelectric materials that have been doped with rare earths. The Rare Earth Team, managed by Dr. Evgenii Levin, found that by adding the equivalent of 1% cerium or ytterbium to the  $\text{Bi}_2\text{Te}_3$  compound, the thermoelectric modules had an improved performance by up to 25% [22].

In addition, the performance improvement of the conventional thermoelectric generators, whose main objective is (i) in combustion vehicles, (ii) in the aerospace industry, (iii) in building installations, and (iv) in electronics industry [4,5,23–50].

This article presents the design and development of a new solid-state generator device using thermoelectric modules, for the experimental analysis of the technical viability of the uses of residual energy (thermal losses) in industrial processes. These processes include forging and hot rolling, industrial refrigeration systems, boilers, ceramic kilns, and the heat that is wasted by the motor of an automobile that can be converted into electricity to charge the batteries. For this purpose, this paper presents the following contributions:

- Modeling and analytical methodology [6] for the design of a thermoelectric generator system (TEGs);
- Prototype of TEGs for waste heat recovery at a low temperature [7]; and
- Prototyping and experimental analysis of the proposed TEGs.

## 2. Methods and Design

In this chapter, we have described the small-scale development of the thermoelectric generator prototype, which was sized from the analytical model that was described by Ando Junior [7]. Then it has presented the electric characterization of the generator, performed by means of an experimental method.

The Figure 1 shows the schematic design of the idealized generator prototype that was classified as a Full Regenerative System, which was aimed at cogeneration of electric energy, through the capture of the dissipated heat (residual energies) of the industrial processes, transforming thermal energy directly into electricity [6].

As it can be seen in Figure 1, the prototype of the thermoelectric generator consisted of two thermal transfer independent systems working jointly. The first system captured the residual heat (3, 4) of the industrial processes, which consisted of a heat transfer module (3) and a heat transfer (hot place) (4), which was responsible for transferring heat (4) by convection from the process to the heat transfer block (3), where the arrangement of the thermoelectric modules (5) was located. In addition, the second system was a hybrid refrigeration-cogeneration set (1, 2, 7, and 8) that was composed of fins (1, 7) and a flat cooling block (2, 8), in order to increase the contact area with the thermoelectric modules, simultaneously obtaining hot water (6), which could have even been reused in the industrial process itself, and warranting a thermal gradient for thermoelectric generation. It should be noted that the thermal system that has been presented allowed for its adaptation to any process by substituting the heat exchanger (4), thus optimizing the thermal transfer to the generator.

Subsequently, the electrical system was preconceived by means of a calculation methodology for the design and electrical dimensioning of generators, based on the Seebeck effect, from the theoretical performance curves of the thermoelectric modules and temperature gradients that were usually found in the industrial processes. It allowed for sizing and conditioning of the signal (power and voltage) that best suited the conditions of operation of the load that was supplied, as well as the operating conditions of any industrial process (temperature gradient), optimizing the power generation.

Therefore, the design and dimensioning of an electric power generator device with a heat transfer system (4), together with the electric calculation methodology, resulted in a prototype of a generator for energy harvesting. It should be noted that the thermoelectric generator was an innovative development

regarding the modular design and reconfigurable topology, which was related to the application in cogeneration.

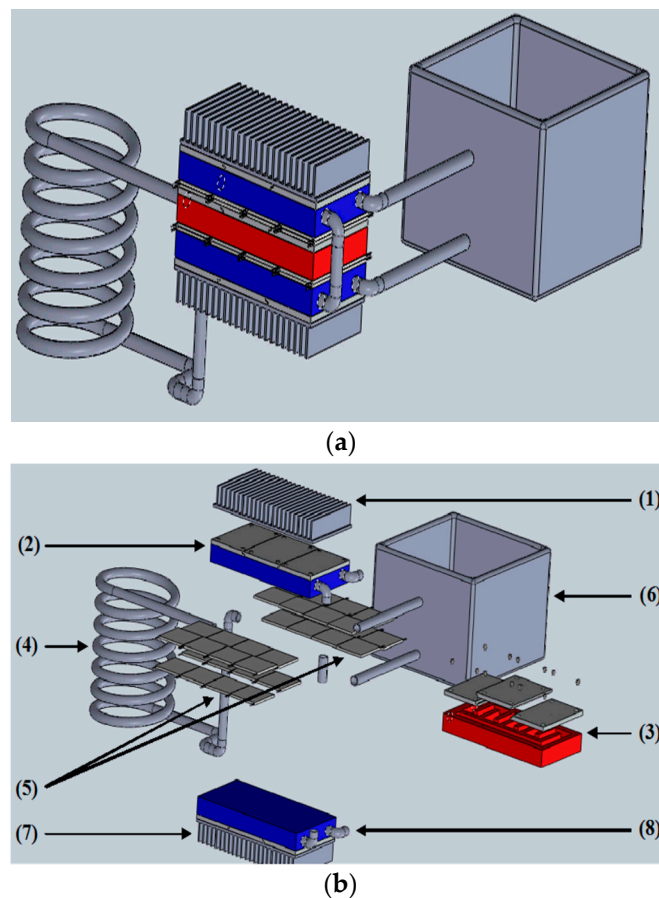


**Figure 1.** Design of the proposed (a) and demonstrated parts and pieces of the generator prototype (b).

### 3. Characterization of TEGs

The solid state thermoelectric generator prototype was dimensioned to serve a load of approximately 40W, with the output voltage of 15VDC for a maximum temperature gradient of 800 °C. For this, 20 thermoelectric modules (model INBC1-127.08HTS, WATRONIX, West Hills, CA, USA) were used in the electrical arrangement that consisted of 10 modules in series, with two associated series sets in parallel, the 20 modules were arranged on both sides of the hot source. Each were composed of ten modules per layer (Figure 1—item 5) [8].

It should be noted that the tests were performed with temperature gradients below the maximum operating limit of the generator system (170 °C), as a result of compliance with laboratory safety standards. For data acquisition purposes, the system was developed and presented in [9] applying the same test methodology used by Ando et al. [10].

#### 3.1. Open Circuit Test

The open circuit test consisted of supplying a given temperature gradient and measuring the thermal quantities (temperature, hot and cold source) and the electrical voltage that was generated at the open output terminals ( $V_{out}$ ), that is, without the load connection at the terminals. Figure 2 shows the graph that was obtained from the results of the open-circuit test, which demonstrated the increase of the output voltage ( $V_{out}$ ) for different temperature gradients ( $\Delta T$ ).

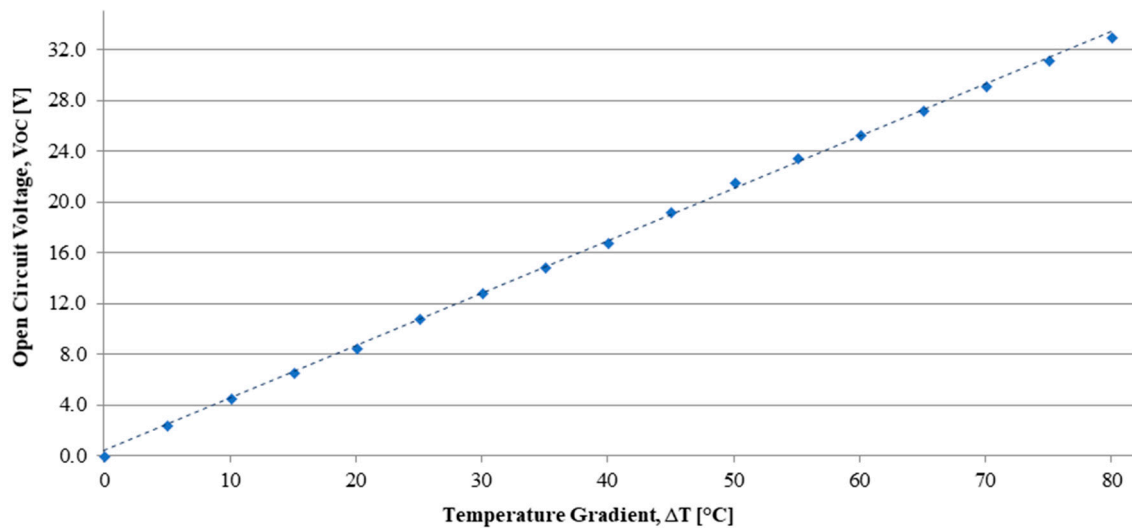


Figure 2. Results obtained in the open circuit test (INBC1-127.08HTS).

Based on Figure 2, it could be seen that the voltage that was generated varied linearly with the temperature gradient. Applying the least squares method for all of the samples of the output voltage ( $V_{out}$ ), we obtained Equation (1), which described the open circuit voltage.

$$V_{out} = 0.4306 \Delta T \text{ (V)} \quad (1)$$

If it was necessary to maintain the output voltage in a fixed value, it is necessary to use a DC-DC converter.

### 3.2. Determination of the Voltage-Current Curve

In order to determine the voltage versus current curve ( $V-I$ ) of the thermoelectric generator, we used a set of resistors as a load to measure the output voltage ( $V_{out}$ ) in (V), compared to the output current ( $I_{out}$ ) in (A), for different temperature gradients ( $\Delta T$ ) ranging from 5 °C up to the predetermined operating limit of 80 °C. The results are shown in Figure 3, dashed lines were obtained by the method of least squares (linear regression), where each one referred to a temperature gradient from 5 °C to 80 °C, in 5 °C intervals.

When analyzing the output voltage ( $V_{out}$ ) curve as a function of the output current ( $I_{out}$ ), shown in Figure 3, for the different temperature gradients ( $\Delta T = T_H - T_C$  (°C)), it could be seen that, analogously to the open-circuit voltage, the increase of both  $V_{out}$  and  $I_{out}$  was directly proportional to the increment of the temperature gradient ( $\Delta T$ ), consequently there was a significant increase in the output power ( $P_{out}$ ) in the presence of higher temperature gradients ( $\Delta T$ ). Figure 3 shows some linearity between the curves for different temperature gradients ( $\Delta T = T_H - T_C$  (°C)). This was because of the fact that the internal resistance ( $R_{int}$ ) of the module had a linear behavior in relation to the test temperature gradient.

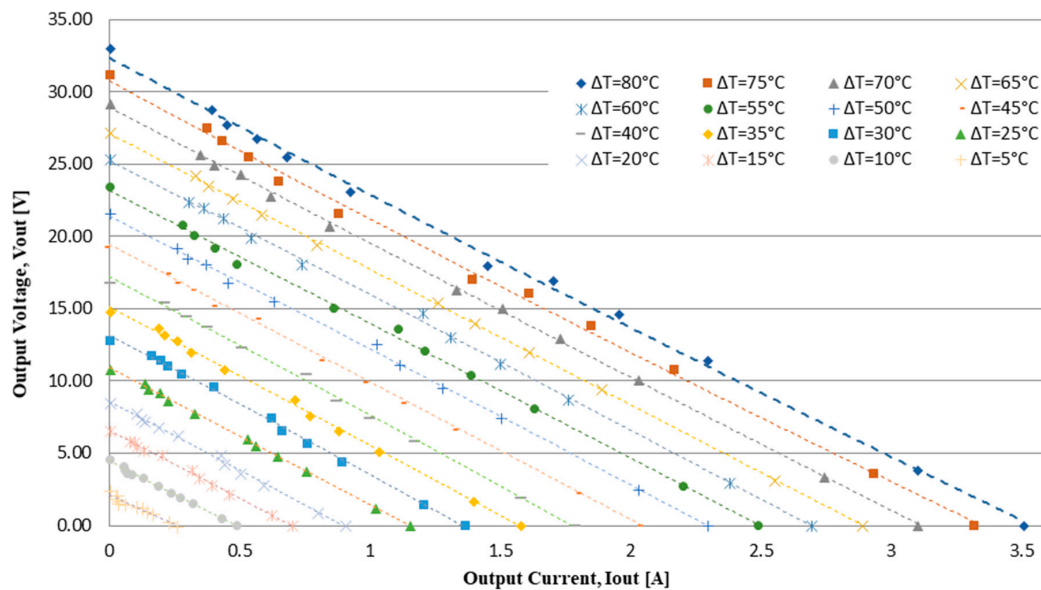


Figure 3. Output voltage vs. output current curve.

### 3.3. Internal Resistance of the TEGs Device

For the determination of the internal resistance of the solid-state thermoelectric generator, we used the data that were obtained in the open circuit test, presented in Figure 2, and the data that were obtained in the test for the determination of the output voltage curve ( $V_{out}$ ) in (V) versus the ( $I_{out}$ ) in (A), shown in Figure 3. Using these data and applying the general theory of circuit analysis, it was possible to obtain the values of the internal resistance ( $R_{int}$ ) samples, measured in ( $\Omega$ ), of the proposed generator for different temperature gradients ( $\Delta T$ ), as shown in Figure 4.

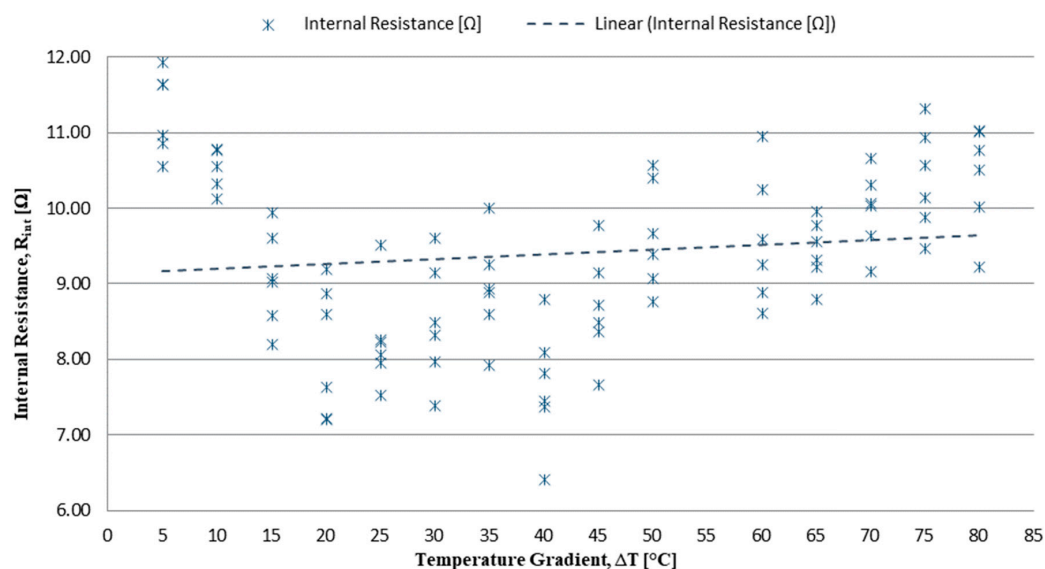
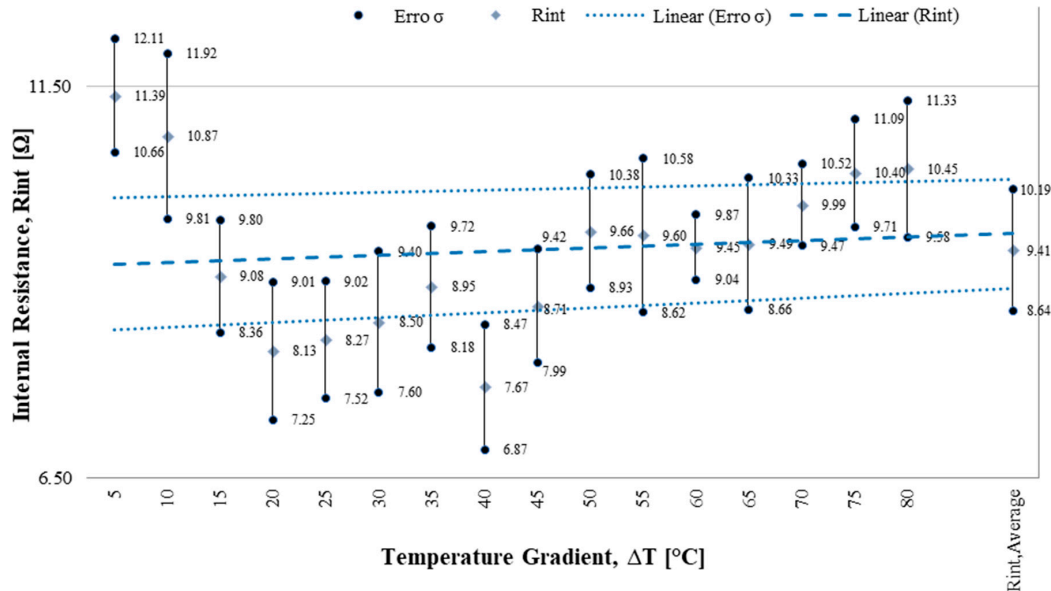


Figure 4. Demonstration of internal resistance ( $R_{int}$ ) samples as measured in the test.

When analyzing the trend line of the samples, it was clear that the internal resistance ( $R_{int}$ ) was directly proportional to the temperature gradient ( $\Delta T$ ).

In order to perform a statistical treatment of the internal resistance ( $R_{int}$ ) samples ( $\Omega$ ) that were measured in the test, the internal resistance ( $R_{int}$ ) was calculated for the different temperature gradients ( $\Delta T$ ) and their respective standard deviations ( $\sigma_n$ ). The mean of the average internal resistance

( $R_{int\_med}$ ) of the entire sample universe was calculated and the respective standard deviation of the sample set ( $\sigma_{med}$ ) was given by the mean of the standard deviations ( $\sigma_n$ ). Figure 5 shows the mean values of internal resistance ( $R_{int}$ ) for different temperature gradients ( $\Delta T$ ) and their respective standard deviations ( $\sigma_n$ ).



**Figure 5.** Internal resistance means ( $R_{int}$ ) for different temperature gradients ( $\Delta T$ ) and their respective standard deviations ( $\sigma_n$ ).

It should be noted that, in Figure 5, the dotted line represented the trend line of the mean internal resistance and its respective standard deviations ( $\pm\sigma$ ), which demonstrated that the internal resistance ( $R_{int}$ ) presented a linear variation with the increase of the temperature gradient ( $\Delta T$ ). While the last bar to the right of the graph labeled 'Average Rint' represented the average resistance values.

The central triangle of the resistance lines' values, in Figure 5, represented the average internal resistance ( $R_{int\_med}$ ) of the entire sample universe ( $R_{int\_med} = (\mu_1 + \mu_2 + \dots + \mu_{15} + \mu_{16})/16 \approx 9.41 \Omega$ ), while the marked edges with a circle symbol at the vertex of the upper and lower line were the standard deviation of the sample set ( $\sigma_{med}$ ), which represented the standard deviation of the set ( $\sigma_{med} = \sigma_1, \sigma_2, \dots, \sigma_{15}, \sigma_{16} \approx 0.77 \Omega$ ), which were equidistant from the center that was demarcated by the triangle, which represented the mean resistance ( $R_{int\_med}$ ).

Consequently, it was possible to state that the internal resistance ( $R_{int\_med}$ ) of the analyzed solid-state thermoelectric generator was equal to the  $R_{int\_med} = 9.41 \Omega$ , with a tolerance equal to  $\Delta R_{int\_med} = 0.77 \Omega$ , that is,  $R_{int} = 41 \pm 0.77 \Omega$ .

### 3.4. TEGs Power Curve

For the determination of the maximum power curve that was transferred by the solid state generator, the data that were obtained in the open circuit test, presented in Figure 2, were used. The data that were obtained in the test for determination of the output voltage–current curve, shown in Figure 3, and the  $R_{int} = R_{int\_média} \pm \Delta R_{int\_med} = 9.41 \pm 0.77 \Omega$ , allowed us to establish a directly proportional relation between the temperature gradient ( $\Delta T$ ) and the power supplied ( $P_{out}$ ) in (W) for a given fixed load,  $R_L$  in ( $\Omega$ ). Therefore, based on the general theory of electrical circuit analysis, we found that the power that was dissipated in the external load would be  $P_{out} = R_L I_{out}^2$  (W). Based on this finding, and using different resistance values as fixed load  $R_L$ , Figure 6 shows the curve of the maximum power that was supplied ( $P_{out}$ ) as a function of the output current ( $I_{out}$ ) for different temperature gradients ( $\Delta T$ ). The graph of Figure 7 shows the maximum output power ( $P_{out}$ ) curve as



a function of the output voltage ( $V_{out}$ ) for different temperature gradients ( $\Delta T$ ). The dashed curves in Figures 6 and 7 were obtained with the help of the lines of the linear regression in Figure 3, by multiplying those values by the current that the module had injected into the load.

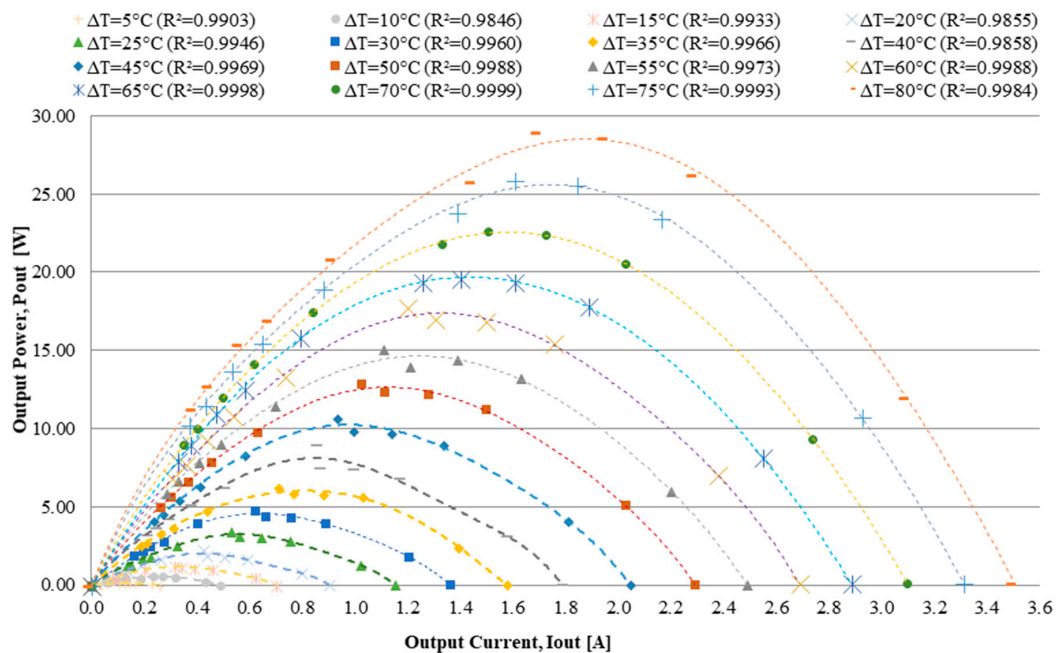


Figure 6. Output power–output current curve.

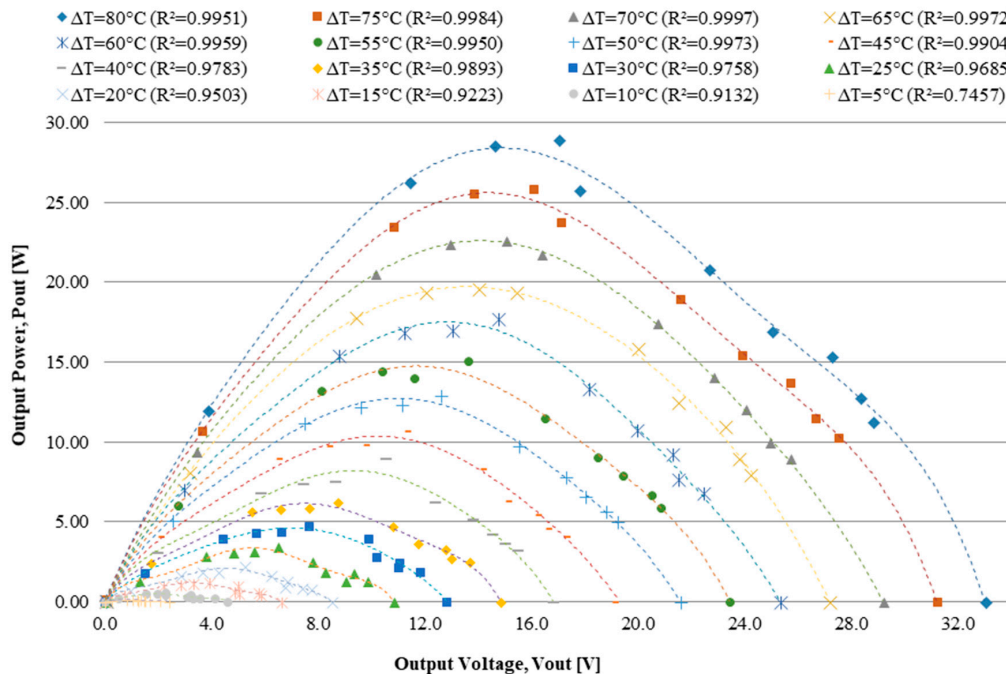


Figure 7. Output power–output voltage curve as function of temperature gradient.

By analyzing the power output ( $P_{out}$ ) curve as a function of the output current ( $I_{out}$ ), shown in Figure 6, it was possible to determine the maximum current and power that were supplied by the thermoelectric generator for different temperature gradients ( $\Delta T$ ). Analogously, the maximum power output ( $P_{out}$ ) and voltage ( $V_{out}$ ) at the output terminals of the solid state thermoelectric generator could

be easily determined by analyzing the data that were provided by the maximum power curve ( $P_{out}$ ), as a function of the voltage of ( $V_{out}$ ), shown in Figure 7, for the different temperature gradients ( $\Delta T$ ).

#### 4. Results and Discussion

The results that were obtained were analyzed and have been discussed in this chapter to make it more comprehensible, and at the same time, to provide information regarding the validation and application of the new proposed generator in other places.

The experimental characterization and validation of the generator experiment, demonstrated consistency with the data that were presented by the authors [11,12]. Their results were validated by a performance analysis by the authors of [8], which was additionally validated by the comparison by the authors of [26,28,30] and other references that were cited throughout this chapter. Other applications of the evaluated technology (TEGs) gave gains of up to 52 W in residential chimneys [51], generation rates of up to 10.9 kWh/m<sup>2</sup> per year in of solar ponds [52], potential power to near 50 W in driving cycle conditions of diesel light-duty engines [53], and allowed efficiencies to reach 55% in proton exchange membrane fuel cells [54].

Based on the data in [8], the prototype solid state thermoelectric generator was sized to be capable of supplying a 40 W power with the 15 V output voltage for an average temperature gradient of 800 °C. However, when analyzing the maximum power curve ( $P_{out}$ ) as a function of the output voltage ( $V_{out}$ ), shown in Figure 7, it could be seen that the generator was capable of supplying approximately 29 W with a voltage of 17 V for a temperature gradient ( $\Delta T$ ) of 80 °C. Therefore, when comparing the experimental results with the theoretical results, it was noticed that the generator that was developed with the thermoelectric module model INBC1-127.08HTS presented a performance below the expected value. It should have been noted that this performance discrepancy was principally as a result of the variation in the contact surface temperature of the modules, which had a temperature gradient difference ( $\Delta T$ ) of up to 7 °C, which was associated with the thermal contact resistance. In addition, the component and surface temperatures were determined by means of spot measurements, using thermocouples (type K) to establish the temperature gradients ( $\Delta T$ ), a strategy that was implemented in response to the physical access limitation of the surfaces of the already coupled device.

The thermoelectric device DT1089 (Marlow Industries Inc., Dallas, TX, USA) at its current best configuration, generated approximately 0.5 W per unit of thermoelectric module for a temperature gradient ( $\Delta T$ ) of 80 °C, still the developed generator produced approximately 1.45 W per unit of thermoelectric module (INBC1-127.08HTS) for a temperature gradient ( $\Delta T$ ) of 80 °C, which represented an energy generation per module increase of about three times.

Based on the maximum power curve ( $P_{out}$ ), as a function of the output voltage ( $V_{out}$ ) (Figure 7) and making an approximation of the values by means of interpolation, it was realized that the developed generator produced about 1.8 W using 20 thermoelectric modules, model INBC1-127.08HTS, for a temperature gradient ( $\Delta T$ ) of 18 °C, occupying a surface area of 320 cm<sup>2</sup>, representing a generation increase of approximately 50% (516 W) compared to the device shown by Azarbayjani et al. [40], per unit surface area. Using low temperature modules would require a higher number, (i.e., more than the 90 modules) were used by Azarbayjani et al. [40]. This difference was principally as a result of the characteristics of the thermoelectric modules that were used in the development of the proposed thermoelectric generator that presented a better performance in the operating range between 40 °C and 170 °C, according to Dalola et al. [5] and the tests that were performed. Therefore, after this analysis, it could be stated that the choice of the thermoelectric modulus that was to be used for the development of a thermoelectric generator should have considered primarily the range of the temperature gradient ( $\Delta T$ ).

When comparing the proposed prototype with devices that operated with relatively high temperature gradients ( $\Delta T$ ), such as the Hi-Z technology system that was presented by Faria et al. [41], which generated 20 W with an output voltage of 12 to 14 V, or the system presented by Nuwayhid et al. [42], which generated 12.6 W using three modules and a surface area of about 430 cm<sup>2</sup>



for a temperature gradient ( $\Delta T$ ) of 152 °C, we found that, from the performance curve of the maximum power ( $P_{out}$ ) as a function of the output voltage ( $V_{out}$ ) (Figure 7), the generator that had developed when it was subjected to a temperature gradient ( $\Delta T$ ) of 152 °C would generate approximately 90 W, with an output voltage between 32 V and 74 V, over a surface area of about 320 cm<sup>2</sup>. Therefore, it could be stated that when the developed prototype was compared with systems such as those presented by Faria et al. and Nuwayhid et al. [41,42], which operated at range of temperature between 40 °C and 170 °C, the prototype presented a satisfactory and superior performance both in ( $P_{out}$ ) as it did in the smallest occupied area.

Using the performance curve of the thermoelectric modulus with the model (INBC1-127.08HTS) being employed, having re-adjusted the theoretical estimate and the correlating the values of the maximum power curve ( $P_{out}$ ) as a function of the output voltage ( $V_{out}$ ) of Figure 7, we found that the generator that had developed when it was subjected to a temperature gradient ( $\Delta T$ ) of 170 °C would generate approximately 107 W, with an output voltage of 36.15 V over a surface area of about 320 cm<sup>2</sup>. Thus, it could be stated that the solid state thermoelectric generator produced results that were consistent with the current state of the art methods, according to the authors of [22,29,35,38]. It presented a similar performance to the thermogenerator that was presented by Riffat et al. [25], which generated 150 W in 12 V and 24 V and was capable of charging batteries and accessories of the automobile, with the output power similar to that of Gao [36], whose multi-mission radioisotope thermoelectric generator (MMRTG) generated 120 W.

From the point of view of application, thermoelectric materials have been widely used in cooling processes, transforming electric energy into thermal energy (Peltier effect) [24,28,30,37]. However, the use of the reversible thermoelectric effect (i.e., transforming thermal energy directly into electrical energy) (Seebeck Effect) had still not been explored much for the purposes of electric energy generation, as shown in [13–15]; in this way, the proposed device provided a valuable contribution to the implementation of this new technology.

When analyzing the proposed thermoelectric generator, within the large scale, it was clear that it could help improve the energy efficiency of the processes and reduce the electrical energy consumption of any system. Moreover, it was possible to adapt the proposed microprocessor to various processes and to obtain high power values, as in the case of a large-scale cogeneration system with high temperature gradients. This technology could be widely used in industry, because there were many processes involving heat exchanges, for example, thermoelectric plants, ceramics, and foundries were identified as industries with a great potential for the application of solid state generators.

It was noteworthy that, despite the difficulties in obtaining thermoelectric materials with high efficiency—that is, high electrical conductivity and low thermal resistance, which was not common in any material, as can be seen from the authors of [55–58]—interest in the development of new thermoelectric materials had recently returned, as they had a promising future, given the need to ensure new sources of clean energy. In conclusion, it could be stated from the authors of [20,34] that this solid-state cogeneration system could be applied in any process involving heat, since even with a low yield of thermoelectric materials as demonstrated by Azarbayjani et al. [40], the result was significant when it was analyzed globally.

Finally, it was verified that, despite the adversities to which the real system was exposed, both in the generation and in the variation of the temperature gradient, as well as in the data collection, the obtained results were satisfactory for an experimental bench prototype and demonstrated the functionality and effectiveness of the solid state thermoelectric generator, a fact that was validated by references and experimental tests, which proved the technical feasibility of using it to capture thermal losses in industrial processes and subsequent generation of electric energy. Therefore, it was an embryonic technology that needed to be developed for large-scale application, and thus in the medium and long term, it would make it a competitive source of clean energy.

## 5. Conclusions

This paper presents the proposal of a generator to capture thermal losses resulting from industrial processes, without affecting the efficiency of the main system, thus characterizing the reuse of residual energy.

According to the principle of conservation of energy, the utilization of part of the thermal wasted energy can be done at the same place that generates this waste. Consequently, reusing part of this residual energy will maximize the yield of the system as a whole. In addition, it is worth noting that the capture of residual energy through the Seebeck effect for energy cogeneration is possible, besides its ease of application, weight, and size, it also contributes to generating electricity in a renewable and clear way. From this, the application of the proposed thermoelectric generator can be made in places such as a thermoelectric plant, where the residual energy resulting from the generation process is easy to capture; in the flue gas exhaust of a vehicle; in industrial heat exchangers; and at forging or forming processes, developments that guarantee an ease of capture in which the presence of the thermoelectric generator does not interfere with the main manufacturing process.

It should be noted that the generator that has been presented will have an important impact on the operation of the industries, as it will enable the improvement of the overall performance of the system through the capture of losses. In addition to the reduction in losses, there is a decrease in the consumption of electricity and fuel, which consequently leads the containment of works to increase generation capacity, thus causing a positive impact in economic terms and socio-environmental issues for both industries and the electricity sector.

The relevance of this mode of electric energy harvest is the fact that it is clean energy and that it depends only on the capture of losses. Those residual energies from industrial processes are, in principle, released to the environment without being exploited. With the proposed invention, the waste energy will not be released into the environment and it will be used for electrical generation and useful heat production.

The results of this research project demonstrated the technical feasibility of the use of thermoelectricity for the capture of thermal losses in industrial processes, having main equipment as the prototype of an energy regeneration system capable of converting thermal energy directly into electric energy by means of the abstraction of residual energy from industrial processes, including for operating with relatively low temperature gradients.

As a continuation of this research, it is proposed that there should be further analysis of the TEG life cycle in industrial processes, as there are currently no studies that address the economic viability and usefulness, because it is a new technology in its design and application.

**Author Contributions:** O.H.A.J. conducted research and participated in the writing and review of the paper; N.H.C. designed of the infrastructure and participated in the writing of the paper; S.S.d.S. did the methodology and participated in paper writing.

**Conflicts of Interest:** The authors declare no conflict of interest.

## References

1. Bastos, S.A.M. *Pulseira para Geração de Energia*. Master's Thesis, Universidade do Minho, Braga, Portugal, 2010.
2. Santos, L.P. *Análise de Desempenho de um Gerador Termoelétrico Baseado no Efeito Seebeck*. Master's Thesis, Universidade de Taubaté, Taubaté, Brazil, 2010.
3. Min, G.; Rowe, D.M. Conversion Efficiency of Thermoelectric Combustion Systems. *IEEE Trans. Energy* **2007**, *22*, 528–534. [[CrossRef](#)]
4. Ono, K.; Suzuki, R.O. Thermoelectric Power Generation: Converting Low-Grade Heat into Electricity. *Energy Resour.* **1998**, *50*, 49–51. [[CrossRef](#)]
5. Dalola, S.; Ferrari, V.; Guizzetti, M.; Marioli, D.; Sardini, E.; Serpelloni, M.; Taroni, A. Autonomous Sensor System with RF Link and Thermoelectric Generator for Power Harvesting. In Proceedings of the International Instrumentation and Measurement Technology Conference, Victoria, BC, Canada, 12–15 May 2008; pp. 12–15.

6. Ando Junior, O.H.; Ferro, J.L.; Schaeffer, L. Desenvolvimento de uma metodologia para dimensionamento elétrico de microgeração de energia elétrica a partir de módulos termoeletricos. In Proceedings of the 3<sup>a</sup> RenoMat—Conferência Internacional de Materiais e Processos para Energias Renováveis, Porto Alegre, Brazil, 9–11 October 2013.
7. Ando Junior, O.H. Microgerador termoeletrico para captação de energia baseado no efeito seebeck com sistema de transferência de calor intercambiável. BR n° BR1020130279471. *Revista da Propriedade Industrial* **2014**, *1*. Available online: <http://hdl.handle.net/10183/174315> (accessed on 6 May 2018).
8. Datasheet inbC1-127.08HTS Thermoelectric Power Generation. Available online: <https://inbthermoelectric.com/wp-content/uploads/2018/02/inbC1-127.0HTS.pdf> (accessed on 24 April 2017).
9. Ando, O.H., Jr.; Izidoro, C.L.; Gomes, J.H.; Carmo, J.P.; Schaeffer, L. Acquisition and Monitoring System for TEG Characterization. *Int. J. Distrib. Sens. Netw.* **2015**, *11*. [CrossRef]
10. Izidoro, C.L.; Ando, O.H., Jr.; Carmo, J.P.; Schaeffer, L. Characterization of Thermoelectric Generator for Energy Harvesting. *Measurement* **2017**, *106*, 283–290. [CrossRef]
11. Carmo, J.P.; Ando, O.H., Jr.; Carmo, J.P.; Schaeffer, L. Characterization of thermoelectric generators by measuring the load-dependence behavior. *Measurement* **2011**, *44*, 2194–2199. [CrossRef]
12. Ando, O.H., Jr.; Ferro, J.L.; Izidoro, C.L.; Maestrelli, E.; Spacek, A.D.; Mota, J.M.; Malfatti, C.F.; Schaeffer, L. Proposal of a Thermoelectric Microgenerator based on Seebeck Effect to Energy Harvesting in Industrial Processes. *Renew. Energy Power Qual. J.* **2014**, *1*, 227–333.
13. Böttner, H.; Nurnus, J.; Gavrikov, A.; Kuhner, G.; Jagle, M.; Kunzel, C.; Eberhard, D.; Plescher, G.; Schubert, A.; Schlereth, K.-H. New Thermoelectric Components Using Microsystem Technologies. *J. Microelectromech. Syst.* **2004**, *3*, 414–420. [CrossRef]
14. Gonçalves, L.M.; Rocha, J.G.; Couto, C.; Alpuim, P.; Correia, J.H. On-Chip Array of Thermoelectric Peltier Microcoolers. *Sens. Actuators A Phys.* **2008**, *145–146*, 75–80. [CrossRef]
15. Ando, O.H., Jr.; Spacek, A.D.; Neto, J.; Oliveira, M.O. Analyze the Potential of Use Thermoelectric Materials for Power Cogeneration by Energy Harvesting—Brazil. *Int. J. Autom. Power Eng.* **2013**, *2*, 303–311.
16. Uchida, K.; Takahashi, S.; Harii, K.; Ieda, J.; Koshibae, W.; Ando, K.; Maekaw, S.; Saitoh, E. Observation of the Spin Seebeck Effect. *Nature* **2008**, *455*, 778–781. [CrossRef] [PubMed]
17. Flipse, J.; Dejene, F.K.; Wagenaar, D.; Bauer, G.E.W.; Youssef, J.B.; van Wees, B.J. Observation of the Spin Peltier Effect for Magnetic Insulators. *Phys. Rev. Lett.* **2014**, *113*, 027601. [CrossRef] [PubMed]
18. Flipse, J.; Bakker, F.L.; Slachter, A.; Dejene, F.K.; van Wees, B.J. Direct Observation of the Spin-Dependent Peltier Effect. *Nat. Nanotechnol.* **2012**, *7*, 166–168. [CrossRef] [PubMed]
19. Gonçalves, L.M.; Couto, C.; Alpuim, P.; Rowe, D.M.; Correia, J.H. Thermoelectric Properties of Bi<sub>2</sub>Te<sub>3</sub>/Sb<sub>2</sub>Te<sub>3</sub> Thin Films. *Mater. Sci. Forum* **2005**, 156–160. [CrossRef]
20. Appel, O.; Zilber, T.; Kalabukhov, S.; Beeri, O.; Gelbstein, Y. Morphological effects on the thermoelectric properties of Ti<sub>0.3</sub>Zr<sub>0.35</sub>Hf<sub>0.35</sub>Ni<sub>1+x</sub>Sn alloys following phase separation. *J. Mater. Chem. C* **2015**, *3*, 11653–11659. [CrossRef]
21. Hazan, E.; Ben-Yehuda, O.; Madar, N.; Gelbstein, Y. Functional Graded Germanium–Lead Chalcogenide-Based Thermoelectric Module for Renewable Energy Applications. *Adv. Energy Mater.* **2015**. [CrossRef]
22. Ritz, F.; Peterson, C.E. Multi-mission radioisotope thermoelectric generator (MMRTG) program overview. In Proceedings of the Aerospace Conference, Big Sky, MT, USA, 6–13 March 2004; p. 2957.
23. Landim, A.L.P.F.; de Azevedo, L.P. O Aproveitamento Energético do Biogás em Aterros Sanitários: Unindo o Inútil ao Sustentável. BNDES Setorial, Rio de Janeiro. 2008. Available online: [https://www.bndes.gov.br/SiteBNDES/export/sites/default/bndes\\_pt/Galerias/Arquivos/conhecimento/bnset/set2704.pdf](https://www.bndes.gov.br/SiteBNDES/export/sites/default/bndes_pt/Galerias/Arquivos/conhecimento/bnset/set2704.pdf) (accessed on 13 May 2018).
24. Nascimento, A.L.E.D.S.; Lubanco, J.C.; Moreira, T.A. Fontes Alternativas de Energia Elétrica: Potencial Brasileiro, Economia e Futuro. Revista de Divulgação do Projeto Universidade Petrobras e Instituto Federal Fluminense, Rio de Janeiro. 2012. Available online: <http://essentiaeditora.iff.edu.br/index.php/BolsistaDeValor/article/viewFile/2391/1280> (accessed on 10 May 2018).
25. Riffat, S.B.; Xiaoli, M. Thermoelectrics: A Review of Present and Potential Applications. *Appl. Therm. Eng.* **2003**, *23*, 913–935. [CrossRef]
26. Alves, P.P. A Experiência de Joule Revisitada. Master’s Thesis, Universidade Nova de Lisboa, Lisboa, Portugal, 2008.

27. Moura, J.A.D.S. Filmes Nanométricos de Fen e Aln Crescidos Por Sputtering e Aplicações do Efeito Peltier. Ph.D. Thesis, Universidade Federal Do Rio Grande Do Norte, Natal, Brazil, 2010.
28. Gonçalves, L.M. Microssistema Termoelétrico Baseado em Teluretos de Bismuto e Antimónio. Ph.D. Thesis, Curso de Engenharia Electrónica Industrial e Computadores, Departamento de Escola de Engenharia, Universidade do Minho, Braga, Portugal, 2008.
29. Gao, M.; Rowe, D.M. Experimental evaluation of prototype thermoelectric domestic-refrigerators. *Appl. Energy* **2006**, *83*, 133–152.
30. Martins, J.; Brito, F.P.; Gonçalves, L.M.; Antunes, J. *Thermoelectric Exhaust Energy Recovery with Temperature Control through Heat Pipes*; SAE Technical Paper; SAE: Warrendale, PA, USA, 2011; pp. 1–23. [[CrossRef](#)]
31. Rowe, D.M. *CRC Handbook of Thermoelectrics*; CRC Press: Boca Raton, FL, USA, 1995.
32. Song, Y. Oxide Based Thermoelectric Materials for Large Scale Power Generation. Master's Thesis, Massachusetts Institute of Technology, Cambridge, MA, USA, 2008.
33. Hendricks, T.; Choate, W.T. *Engineering Scoping Study of Thermoelectric Generator Systems for Industrial Waste Heat Recovery*; U.S. Department of Energy, Industrial Technologies Program: Washington, DC, USA, 2006.
34. Ota, T.; Tokunaga, C.; Fujita, K. Development of thermoelectric power generation system for industrial furnaces. In Proceedings of the International Conference on Thermoelectrics, Clemson, SC, USA, 19–23 June 2005; pp. 335–338.
35. Ismail, B.I.; Ahmed, W.H. Thermoelectric Power Generation Using Waste-Heat Energy as an Alternative Green Technology. In *Recent Patents on Electrical Engineering*; Bentham Science Publishers Ltd: Potomac, MD, USA, 2009; pp. 27–39.
36. Gao, M. *Thermoelectric Energy Harvesting*; Artech House: Norwood, MA, USA, 2010; Volume 413–414, pp. 325–336.
37. Fairbanks, J. Vehicular Thermoelectric Applications. In Proceedings of the 6th European Conference on Thermoelectrics, Paris, France, 2–4 July 2008.
38. Romani, R. Aplicações de Efeitos Termoelétricos da Indústria Aeronáutica. In *Congresso Iberoamericano De Engenharia Mecânica*; Pontificia Universidad Catolica del Peru: Cusco, Peru, 2007. Available online: <http://congreso.pucp.edu.pe/cibim8/pdf/29/29-14.pdf> (accessed on 6 June 2018).
39. Huang, J. Aerospace and aircraft thermoelectric application. Boeing Research and Technology. Engineering, Operations, & Technology, U.S. Department Energy. Available online: [https://www1.eere.energy.gov/vehiclesandfuels/pdfs/thermoelectrics\\_app\\_2009/thursday/huang.pdf](https://www1.eere.energy.gov/vehiclesandfuels/pdfs/thermoelectrics_app_2009/thursday/huang.pdf) (accessed on 13 May 2018).
40. Azarbayjani, M.; Anderson, J. Assessment of Solar Energy Conversion Technologies-Application of Thermoelectric Devices in Retrofit Office Building. In Proceedings of the Sixteenth Symposium on Improving Building Systems in Hot and Humid Climates, Plano, TX, USA, 15–17 December 2008.
41. Faria, S.R.A. Protótipo de um Microgerador Termoelétrico de Estado Sólido: Cogeração a Gás. Master's Thesis, Universidade Federal do Rio Grande do Norte, Natal, Brazil, 2009.
42. Nuwayhid, R.; Shihadeh, A.; Ghaddar, N. Development and testing of a domestic woodstove thermoelectric generator with natural convection cooling. *Energy Conver. Manag.* **2004**, *46*, 1631–1643. [[CrossRef](#)]
43. Snyder, G.J. Small Thermoelectric Generators. *Electrochem. Soc. Interface* **2008**, *17*, 54–56.
44. Seiko Instruments Inc. (Japan). *Engineers Pursuing the Ultimate in the Evolution of Wristwatch Technology. Nature Interface*. 2001. Available online: <http://www.natureinterface.com/e/ni03/P045-049/> (accessed on 13 May 2018).
45. Dalola, S.; Ferrari, M.; Ferrari, V.; Guizzetti, M.; Marioli, D.; Taroni, A. Characterization of Thermoelectric Modules for Powering Autonomous Sensors. *IEEE Trans. Instrum. Meas.* **2007**, *58*, 99–107. [[CrossRef](#)]
46. Harb, A. Energy harvesting: State-of-the-art. *Renew. Energy* **2011**, *36*, 2641–2654. [[CrossRef](#)]
47. Gyselinckx, B.; Van Hoof, C.; Ryckaert, J.; Yazicioglu, R.F.; Fiorini, P.; Leonov, V. Human++: Autonomous wireless sensors for body area networks. In Proceedings of the Custom Integrated Circuits Conference, San Jose, CA, USA, 18–21 September 2005; pp. 13–19.
48. Penders, J.; Gyselinckx, B.; Vullers, R.; De Nil, M.; Nimmala, V.; Van De Molengraft, J.; Yazicioglu, F.; Torfs, T.; Leonov, V.; Merken, P.; et al. Human++: From technology to emerging health monitoring concepts. In Proceedings of the 5th International Summer School and Symposium on Medical Devices and Biosensors, Hong Kong, China, 1–3 June 2008; pp. 94–98.
49. Wang, Z.; Leonov, V.; Fiorini, P.; van Hoof, C. Realization of a wearable miniaturized thermoelectric generator for human body applications. *Sens. Actuators A Phys.* **2009**, *156*, 95–102. [[CrossRef](#)]

50. Omer, S.A.; Infield, D.G. Design optimization of thermoelectric devices for solar power generation. *Sol. Energy Mater. Sol. Cells* **1998**, *53*, 67–82. [[CrossRef](#)]
51. Jaber, H.; Ramadan, M.; Lemenand, T.; Khaled, M. Domestic thermoelectric cogeneration system optimization analysis, energy consumption and CO<sub>2</sub> emissions reduction. *Appl. Therm. Eng.* **2018**, *130*, 279–295. [[CrossRef](#)]
52. Ding, L.; Akbarzadeh, A.; Tan, L. A review of power generation with thermoelectric system and its alternative with solar ponds. *Renew. Sustain. Energy Rev.* **2018**, *81*, 799–812. [[CrossRef](#)]
53. Yáñez, P.F.; Gómez, A.; Contreras, R.G.; Armas, O. Evaluating thermoelectric modules in diesel exhaust systems: Potential under urban and extra-urban driving conditions. *J. Clean. Prod.* **2018**, *182*, 1070–1079. [[CrossRef](#)]
54. Kwan, T.H.; Wu, X.; Yao, Q. Multi-objective genetic optimization of the thermoelectric system for thermal management of proton exchange membrane fuel cells. *Appl. Energy* **2018**, *217*, 314–327. [[CrossRef](#)]
55. Goncalves, L.M.; Alpuim, P.; Min, G.; Rowe, D.M.; Couto, C.; Correia, J.H. Optimization of Bi<sub>2</sub>Te<sub>3</sub> and Sb<sub>2</sub>Te<sub>3</sub> thin films deposited by co-evaporation on polyimide for thermoelectric applications. *Vacuum* **2008**, *82*, 1499–1502. [[CrossRef](#)]
56. Polozine, A.; Schaeffer, L. Materiais sintetizados para geração de energia elétrica. In Proceedings of the 3<sup>o</sup> RenoMat—Conferência Internacional de Materiais e Processos para Energias Renováveis, Porto Alegre, RS, Brazil; 2013. Available online: <http://www.ufrgs.br/ldtm/publicacoes/Polozine%20Artigo%20para%20o%20SENAFOR%202013.pdf> (accessed on 6 May 2018).
57. Goncalves, L.M.; Rocha, J.G.; Couto, C.; Alpuim, P.; Min, G.; Rowe, D.M.; Correia, J.H. Fabrication of flexible thermoelectric microcoolers using planar thin-film technologies. *J. Micromech. Microeng.* **2007**, *17*, 7. [[CrossRef](#)]
58. Goncalves, L.M.; Couto, C.; Alpuim, P.; Rowe, D.M.; Correia, J.H. Thermoelectric microstructures of Bi<sub>2</sub>Te<sub>3</sub>/Sb<sub>2</sub>Te<sub>3</sub> for a self-calibrated micro-pyrometer. *Sens. Actuators A Phys.* **2006**, *130–131*, 346–351. [[CrossRef](#)]



© 2018 by the authors. Licensee MDPI, Basel, Switzerland. This article is an open access article distributed under the terms and conditions of the Creative Commons Attribution (CC BY) license (<http://creativecommons.org/licenses/by/4.0/>).